Food Chemistry 331 (2020) 127208

Contents lists available at ScienceDirect

Food Chemistry

journal homepage: www.elsevier.com/locate/foodchem

Short communication

A visual Hg^{2+} detection strategy based on distance as readout by G-quadruplex DNAzyme on microfluidic paper

Chao Wu[a], Guizhen Gao[a], Kefeng Zhai[a], Lisheng Xu[a], Dagan Zhang[a,b,*]

[a] Suzhou Engineering and Technological Research Center of Natural Medicine and Functional Food, School of Biology and Food Engineering, Suzhou University, Suzhou 234000, China

[b] Guangdong Key Laboratory of Biomedical Measurements and Ultrasound Imaging, Department of Biomedical Engineering, Shenzhen University, Shenzhen 518060, China

ARTICLE INFO

Keywords:
Distance
G-quadruplex DNAzyme
Hg^{2+} detection
Paper-chip

ABSTRACT

In this work, we have developed a simple, fast and visual Hg^{2+} detection strategy based on distance as readout on paper chip by the Hg^{2+}-mediated formation of G-quadruplex-hemin DNAzymes. In the presence of Hg^{2+}, the two oligonucleotides hybridize to form G-quadruplex DNA by T-Hg^{2+}-T base pair, which was able to bind hemin to form the catalytically active G-quadruplex-hemin DNAzymes. Once DNAzymes were added to react with the precipitated 3,3,5,5-tetramethyl benzidine (TMB) immobilized on the sample area, a visible color band was produced, and the formed length was positively correlated with the concentration of Hg^{2+}. This biosensor is capable of selectively detecting mercuric ions with good reproducibility and satisfactory dynamic range. The limit of detection was low to 0.23 nM. Therefore, this strategy not only provides a visual and quick screen of Hg^{2+}, but also shows a promising future in monitoring analysis of other metal ions in POC diagnostic field.

1. Introduction

Mercury (Hg) is a hazardous heavy metal contaminant of significant public health concern and occurs widely in water, soil, and even food (Clarkson, 1993; Tchounwou, Ayensu, Ninashvili, & Sutton, 2003). In aquatic ecosystems, Hg is found in elemental, inorganic, and organic forms. Due to microbial methylation, solvated Hg^{2+} converted into methyl mercury, the most toxic form of Hg. Bioaccumulation of Hg in aquatic food chains may cause high levels of Hg contamination in carnivorous fish. Human exposure to Hg occurs largely through the consumption of these contaminated fish. Toxicology studies indicated that elevated Hg in human blood and tissue could cause various severe health problems, including motor skill impairment, reduced reproductive success, hormonal changes, and kidney failure (Moneta, 2009; Streets et al., 2011; Liu, Huang, & Chang, 2009). In addition, Hg is also toxic to the human embryo and fetus. Thus, it is necessary to develop a fast, economical and easy method to monitor aqueous Hg^{2+} ion. At present, traditional detection methods for Hg^{2+} include atomic fluorescence spectrometry (AFS), atomic absorption/emission spectrometry (AAS/AES), and inductively coupled plasma mass spectrometry (ICP-MS) (Zhong, Deng, He, Ge, & Song, 2015; Xu et al., 2015). Although these techniques have high selectivity and accuracy, they require time-consuming sample preparation and complex detection processes, and trained personnel. Moreover, the instrument itself is very expensive and not suit for point-of-care test (POCT). Since G-quadruplex DNA-hemin system was reported, they have been widely used in biosensors for detecting Hg^{2+} (Li, Dong, & Wang, 2009; Li, Li, Wang, & Dong, 2009; Jia, Liu, Li, Kong, & Shen, 2011; Ren, Zhang, Huang, Li, & Luo, 2015; Saidur, Aziz, & Basirun, 2017; Xiong et al., 2019). G-quadruplex consensus sequence consist of four stretches of at least three guanines (G) separated by 1–7 random nucleotides (N), such as the sequence GGGN1-7GGGN1-7GGGN1-7GGG. G-quadruplex DNA can bind tightly to hemin to form the peroxidase mimicking hemin- G-quadruplex DNA complex. For convenience, the hemin–G-quadruplex DNA complex is abbreviated to DNAzyme in the following part. Other Hg^{2+} detection methods based on DNAzyme have also emerged, such as colorimetric analysis, fluorescence analysis, and electrochemical analysis (Wang, Heon Lee, & Lu, 2008; Ren et al., 2016; Cai, Xie, Zhang, Tang, & Tang, 2017; Yun et al., 2017). Among these methods, colorimetric analysis is extremely attractive, because it can be easily read out with the naked eye in POCT. However, color hue and brightness perception may differ from person to person, increasing measurement uncertainty for quantitative detection. Therefore, there is an urgent need to develop a more simple and effective detection method that can be used under resource-limited conditions.

Towards this goal, microfluidic paper-based analytical devices, or μPADs, have shown promise for overcoming technical obstacles (Gao, Liu, & Gu, 2016; Zhang, Gao, Chen, & Liu, 2018, Zhang, Ma, Tang, &

* Corresponding author.
E-mail address: zhang_dagan@126.com (D. Zhang).

https://doi.org/10.1016/j.foodchem.2020.127208
Received 29 August 2019; Received in revised form 27 May 2020; Accepted 31 May 2020
Available online 03 June 2020

Liu, 2018). The detection based on distance is an instrumental-free and simple signal readout method, which was often applied in quantitative analysis in PADs. Generally, colorimetric reagents are previously deposited along the capillary flow path of the paper and can react with analyte. As flowing analyte reacts with reagent, color develops along the flow line. Thus, quantification is obtained by measuring color length on the paper. Distance-based paper devices have been widely used so far. Henry and coworkers developed a quantitative method for detecting small molecular targets and metal ions based on distance readout (Cate, Dungchai, Cunningham, Volckens, & Henry, 2013). Yang and coworkers also reported a series of methods for determining small molecules and proteins by the integration of cellulose paper and functional nucleic acids based on distance readout (Wei et al., 2016; Tian et al., 2017; Liu et al., 2017; Ma et al., 2016). Among most methods based on distance as readout, enzyme is always involved. However, the applications of natural enzymes are limited, because they are sensitive to environmental conditions and remain too costly to produce on a large scale. Furthermore, in most enzyme-catalyzed reactions, 3, 3′-diaminobenzidine (DAB) was used as substrate for distance detection in the presence of peroxidase. However, DAB has strong carcinogenicity and is harmful to operators. It is thus urgent to develop an enzyme-free and non-toxic substrate method for Hg^{2+} detection based on distance as readout. 3,3,5,5-tetramethyl benzidine (TMB) and peroxide (H_2O_2) reaction system is commonly used in chromogenic assay because TMB is non-carcinogenic and colorless. Nevertheless, TMB should be operated carefully because it may cause skin sensitization to person and long-term adverse effects in the aquatic environment.

In this work, we designed a novel method for Hg^{2+} detection by measuring color length formed by oxidation products of TMB on paper chips. Integrating the excellent DNAzyme on the surface of paper chip for visual Hg^{2+} screening based on distance readout has never been implemented. Owing to the high peroxidase-like characteristic, the DNAzyme complex catalyzes the reaction of TMB and H_2O_2 to produce colored products (Gao, Wu, & Gao, 2011). As shown in Fig. 1, the precipitated TMB is loaded onto the paper strip biosensor in advance. In the presence of Hg^{2+}, the probe A and B can turn into the G-quadruplex DNA. Then it binds hemin to form the DNAzyme, which reacts with the precipitated TMB, producing a visible color band on the paper. The color length is proportional to the concentration of $Hg^{2+}$when the concentrations of TMB and H_2O_2 were kept constant. The novel method based on distance readout visual platform for Hg^{2+} detection was also demonstrated in real samples and showed that the detection limit could be as low as 0.23 nM. This method provided a simple, visual and enzyme-free amplification platform for quick and sensitive detection of Hg^{2+}, and our strategy had potential applications in point-of care (POC) diagnostics field.

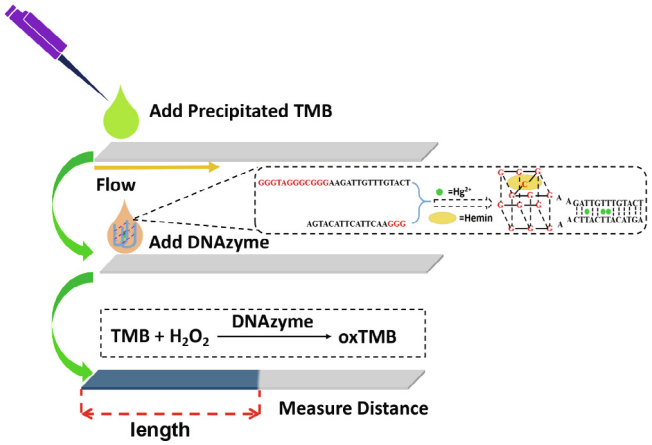

Fig. 1. Schematic Illustration Showing the Based on Distance Assay for the Quantification of Hg^{2+} by G-quadruplex DNAzyme on Paper Chip.

2. Experimental methods

2.1. Materials and reagents

Whatman chromatography paper #1 (WCP#1) (200.0 mm × 200.0 mm), hemin, Tris were purchased from Sigma-Aldrich (Shanghai, China). The probe A (GGGTAGGGCGGGAAGATTG TTTGTACT) and the probe B (AGTACATTCATTCAAGGG) were synthesized by Sangon Biotech (Shanghai, China). 3,3′,5,5′-tetramethylbenzidine substrate solution was purchased from Tiangen Biotech Co.,Ltd (Beijing, China). Metal salts and other chemicals were obtained from Sinopharm Chemical Reagent Co., Ltd (Shanghai, China). The optical scanner (BenQK802) with 1200 × 1200 dpi was from BenQ Company (Shanghai, China). Standard solutions of all metal ions were prepared in deionized water as stock solutions (10 mM). All oligonucleotides were synthesized and purified by Thermo Fisher Scientifc Co., Ltd (Shanghai, China). All reagents were used as received without further purification.

2.2. Synthesis of the DNAzyme complex

The DNA probe A and B were dissolved in Tris-EDTA buffer (10 mM Tris-HCl, 100 mM EDTA, pH = 8.0), with a final concentration of 100 μM. The mixture solution containing 5.0 μL of probe A (10 μM), 5.0 μL of probe B (10 μM) in 10 mM Tris-HCl, 50 mM KCl buffer (pH = 7.4) was heated at 95 °C for 5 min, and then cool slowly back to room temperature (~2.0 h). And then different concentration of Hg^{2+} was added to this mixture solution, and the mixture was allowed to incubate at 25 °C for 30 min. Next, 2.0 μL of hemin solution (2.0 μM) was added to the solution, followed by a 30 min incubation at room temperature to produce the DNAzyme. Visual colorimetric measurement assay was carried out subsequently to this complex formation. 10 μL aliquots of TMB substrate reagent solutions were added to tubes, and then 2.0 μL aliquots of DNAzymes was added and mixed.

2.3. Optimization of conditions

The influences of reaction time were tested as follows: 10 μM probe A and 10 μM probe B were put in pH 7.4 buffer (10 mM Tris-HCl, 50 mM KCl). 200 nM Hg^{2+} was used to test the system. The mixture was incubated from 0 to 30 min, and subsequently 2.0 μM hemin was added. Then, paper was cut into 30 mm × 1.5 mm strips by a laser carve, and then 5.0 μL TMB solution was firstly immobilized at the strips and dried, and subsequently the formed mixture solution was added onto the paper chip and incubated for 5 min. Finally, all the samples were measured by based on distance on paper chip.

2.4. The utility of the biosensor for detecting Hg^{2+}

Paper chips, immobilized by TMB solution, were used to detect Hg^{2+}. Different concentrations of Hg^{2+} (0 nM, 1.0 nM, 5.0 nM, 10 nM, 25 nM, 50 nM, 100 nM and 200 nM) were used to produce the DNAzyme as previously mentioned in Section 2.2.

Then, 5.0 μL of the mixture solutions containing different concentrations of DNAzyme were respectively added onto 30 mm × 1.5 mm paper chips and dried for 5.0 min. Finally, an office scanner (BenQK802) with 1200 × 1200 DPI was used to obtain optical images of the paper chip device to measure distance on paper chip.

2.5. Specifity detection of Hg^{2+}

The specifity for Hg^{2+} was evaluated from a variety of environmentally relevant metal ions, such as K^+, Na^+, Cu^{2+}, Pb^{2+}, Mn^{2+}, Mg^{2+}, Fe^{2+}, Zn^{2+}. The concentrations of Hg^{2+} and other metal ions used in the study were 50 nM and 5.0 mM respectively. And the mixture of Hg^{2+} (50 nM) with different competing metal ions (each

5.0 mM) was also tested as a control.

2.6. Detection of Hg^{2+} in real samples

Five filter water samples were spiked with a series of concentrations of Hg^{2+} (5.0 nM, 10 nM, 25 nM, 50 nM and 100 nM). The mean value and standard deviation and recovery of each sample were calculated accordingly.

3. Results and discussion

3.1. Hg^{2+} detection principle of this strategy

The design and working principle of the detection of Hg^{2+} based on distance as readout on microfluidic paper by DNAzyme was illustrated in Fig. 1. The precipitated TMB was firstly immobilized on the paper strip biosensor. Once the Hg^{2+} appeared, the G-quadruplex DNA was formed based on T-Hg^{2+}-T interaction, which then bound hemin to form the DNAzyme. It was subsequently introduced into paper chips to catalyze the oxidation of TMB in the presence of H_2O_2. Finally, insoluble oxidation products of TMB (oxTMB) formed and deposited on the straight channel and did not migrate with the flow, leading to visualized distance on the paper chip. For a given hemin concentration, the activity of DNAzyme depends on the level of Hg^{2+}. Higher concentrations of Hg^{2+} lead to more DNAzymes, producing more oxTMB when the TMB and H_2O_2 were kept constant. Therefore, the color length is proportional to the concentration of Hg^{2+}. The results of the assay were observed by the naked eye and the color lengths were then measured. This method provided a simple and fast platform for visualized and quantitative detection of Hg^{2+}.

3.2. Feasibility test

To demonstrate the feasibility of our method, the absorption peaks of two kind of samples were measured. The sample B are the mixture of DNAzyme and the TMB substrate reagent solution, while Hg^{2+} is lacking in the sample A, which contained two probes, hemin and TMB substrate reagent solutions. As show in Fig. 2a, in the absence of Hg^{2+}, no characteristic absorption peak at 652 nm was observed in the sample A. The reason for this may be that G-quadruplex DNA failed to form without Hg^{2+}, so the oxidation of TMB did not happen. However, with the help of Hg^{2+}, the probe A and B combined to be the G-quadruplex DNA, which could bind hemin and catalyze TMB to oxTMB polymers. Therefore, an obvious characteristic absorbance peak at 652 nm was found in sample B.

To further identify such principle of the distance detection based on the DNAzyme and TMB system, SEM images of TMB reacted with DNAzyme on paper chips were obtained. As shown in Fig. 2b, on paper with TMB only, almost no cracks between fibers were blocked. In contrast, on the paper with TMB and DNAzyme, the paper surface was filled with oxTMB polymers, and the cracks between fibers were almost blocked by the polymers. (Fig. 2c). Besides, the SEM image of only the blank paper (with no polymers/no Hg) was shown in Fig. S1 and there were big cracks between fibers. These results indicated that color distances were attributed to the formation of oxTMB polymers.

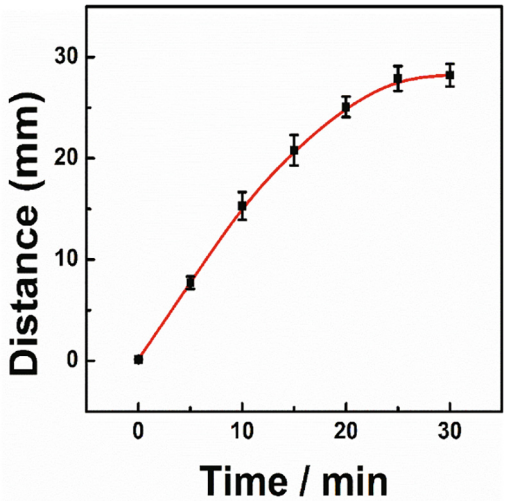

Fig. 3. The relationship of the distance and the reaction time.

3.3. Optimization of the experimental condition

Moreover, we optimized the concentration of reaction time. Incubation time was also an important parameter for the experiment performance. As shown in Fig. 3, the distance readout rapidly increased from 0 to 25 min, and subsequently nearly remained constant and reached a plateau after 30 min. Therefore, we chosen 30 min as optimization incubation time to complete reaction in this study.

3.4. Quantitative detection of Hg^{2+}

Under the optimal conditions, different concentrations of Hg^{2+} (0 nM, 1.0 nM, 5.0 nM, 10 nM, 25 nM, 50 nM, 100 nM and 200 nM) were examined using the proposed strategy. As shown in Fig. 4a, the signal of distance was boosted with the Hg^{2+} concentrations increasing in the range of 0–200 nM, and it was linearly correlated to the logarithm of Hg^{2+} concentration from 1.0 to 50 nM (Fig. 4b). The distance signal reached a maximum when the target concentration reached 200 nM. The limit of detection (LOD), calculated as three times the standard deviation of the blank divided by the slope, was 0.23 nM, which was in accordance with the values previously reported (Apilux, Siangproh, Praphairaksit, & Chailapakul, 2012). The reproducibility of the testing method was also acceptable, which was demonstrated by successively replicated tests in a week (Fig. S2). These results

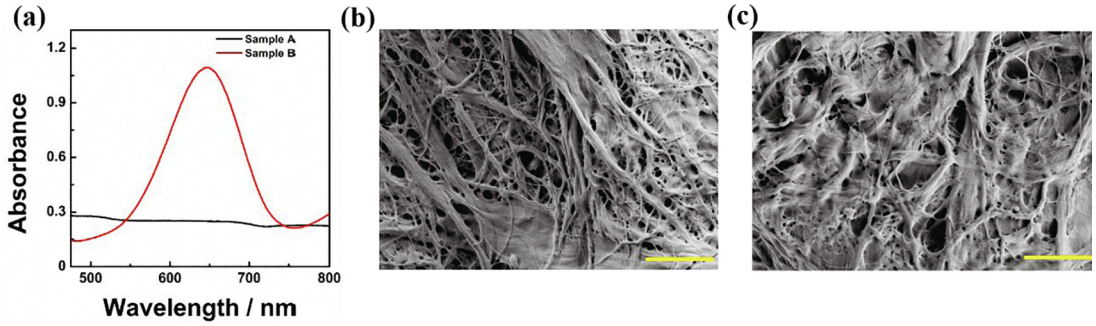

Fig. 2. (a) The characteristic absorption peaks at 652 nm of the sample A and B. (b) SEM images of the TMB reacted with no DNAzyme on the paper surface (c) SEM images of the TMB reacted with Hg^{2+}-induced DNAzyme on the paper surface. Scale bar is 2.0 μm.

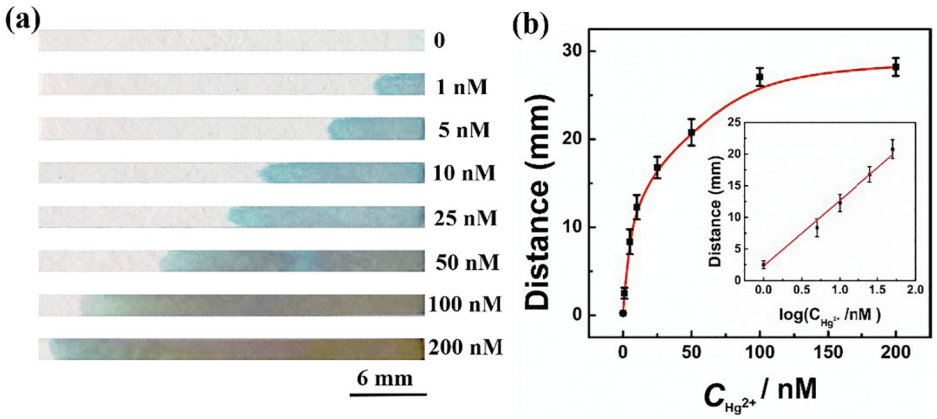

Fig. 4. (a) Optical photographs of different concentrations of Hg^{2+} on paper strips. The concentration of Hg^{2+} in the sample is indicated. (b) Distance of the colored band as a function of Hg^{2+} concentration. Inset: the distance as a function of logarithm of the Hg^{2+} concentration. The error bars represent standard deviation for three replicated measurements.

demonstrated that Hg^{2+} can be quantified based on the length of paper strips. In addition, two different colors were observed on the paper chip at different Hg^{2+}concentrations. According to Gao' study, increasing the concentration of HRP leads to different oxTMB and makes the color change from blue to yellow (Gao et al., 2011). In our study, when the concentrations of Hg^{2+} were more than 50 nM, brown were observed on the paper strips, showing a higher activity of DNAzyme. This was a further evidence of a positive correlation between the concentrations of Hg^{2+} and the activity of the DNAzyme.

3.5. Specificity evaluation

Specificity of detection is a very important parameter for assessment of performance of new method. To validate the specificity of this biosensor, several other metal ions, including K^+, Na^+, Cu^{2+}, Pb^{2+}, Mn^{2+}, Mg^{2+}, Fe^{2+}, Zn^{2+} were tested as controls. And the mixture of Hg^{2+} (50 nM) with different competing metal ions (each 5.0 mM) was also tested as a control, and Hg^{2+} (50 nM) standard solution as positive control (PC). As shown in Fig. 5, only in the presence of Hg^{2+} can induce a remarkable increase in the distance signal. In addition, when Hg^{2+} was incubated with other ions, the coexistence of other metal ions did not apparently affect the Hg^{2+} detection. Therefore, these results indicated that our method had good specificity and could be used for quantification of Hg^{2+}.

3.6. Application in real sample assay

Lastly, the applicability of this method was further evaluated by testing a real sample. Then the filtered water was spiked with a series of concentrations of Hg^{2+} (5 nM, 10 nM, 25 nM, 50 nM and 100 nM as the final concentrations). As shown in Fig. 6, the recovery values ranged from 85.6 to 111.2% and relative standard deviations of the triplicate measurements for all samples were all less than 9.5%. We also chose lake water, tap river and river water as real samples for recovery test, as shown in Fig. S3. These indicated that this proposed bio-sensor was able to detect Hg^{2+} with good accuracy.

4. Conclusions

In summary, a simple, fast and visual Hg^{2+} detection strategy was developed based on distance as readout on paper chip by G-quadruplex DNAzyme. This method offered an enzyme-free and visible readout platform for sensitive detection of Hg^{2+}. This method also showed good selectivity and reproducibility for Hg^{2+} detection and the limit of detection was low to 0.23 nM. Therefore, this strategy showed a promising future in monitoring detection of Hg^{2+} in POC diagnostic field.

CRediT authorship contribution statement

Chao Wu: Data curation, Formal analysis, Writing - original draft. **Guizhen Gao:** Formal analysis, Writing - original draft. **Kefeng Zhai:**

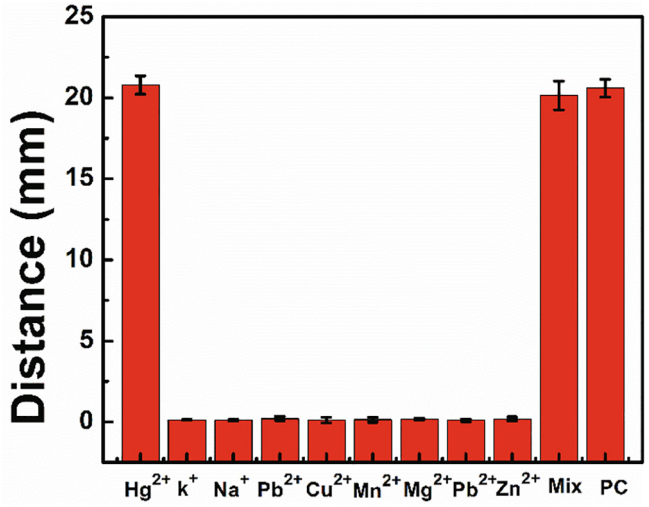

Fig. 5. The specificity of the proposed biosensor for Hg^{2+} over other common metal ions.

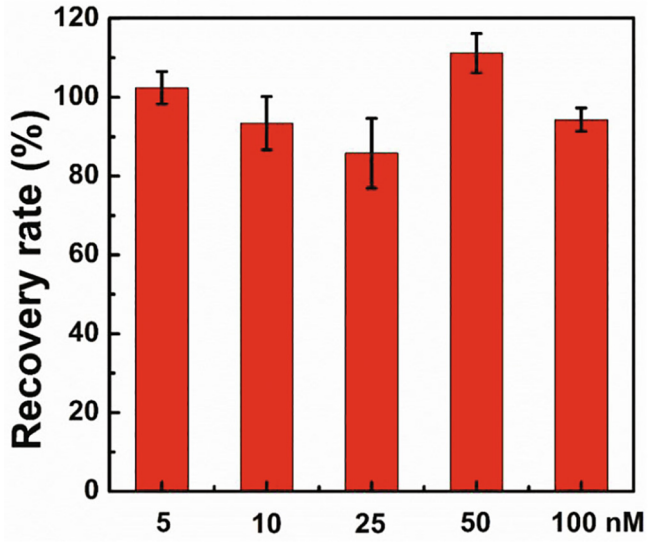

Fig. 6. Recovery rate test of Hg^{2+} in real samples, and the error bars represent standard deviation for three replicated measurements.

Methodology, Investigation, Resources, Funding acquisition, Project administration. **Lisheng Xu:** Methodology, Investigation, Resources, Funding acquisition, Project administration. **Dagan Zhang:** Conceptualization, Methodology, Writing - review & editing, Supervision.

Declaration of Competing Interest

The authors declare that they have no known competing financial interests or personal relationships that could have appeared to influence the work reported in this paper.

Acknowledgements

This work was supported by the National Natural Science Foundation of China (grants 81601034), the Suzhou Engineering and Technological Research Center of Natural Medicine and Functional Food (grants SZ2017ZX06), the Suzhou science and technology plan project (grants SZ2017GG18).

Appendix A. Supplementary data

Supplementary data to this article can be found online at https://doi.org/10.1016/j.foodchem.2020.127208.

References

Apilux, A., Siangproh, W., Praphairaksit, N., & Chailapakul, O. (2012). *Talanta, 97*, 388–394.
Cai, W., Xie, S., Zhang, J., Tang, D., & Tang, Y. (2017). *Biosensors & Bioelectronics, 98*, 466–472.
Cate, D. M., Dungchai, W., Cunningham, J. C., Volckens, J., & Henry, C. S. (2013). *Lab on a Chip, 13*(12), 2397–2404.
Clarkson, T. W. (1993). *Environmental Health Perspectives, 100*, 31–38.
Gao, L., Wu, J., & Gao, D. (2011). *ACS Nano, 5*(8), 6736–6742.
Gao, B., Liu, H., & Gu, Z. (2016). *Analytical Chemistry, 88*(10), 5424–5429.
Jia, S., Liu, X., Li, P., Kong, D., & Shen, H. (2011). *Biosensors & Bioelectronics, 27*(1), 148–152.
Li, T., Dong, S., & Wang, E. (2009). *Analytical Chemistry, 81*(6), 2144–2149.
Li, T., Li, B., Wang, E., & Dong, S. (2009). *Chemical Communications (Cambridge, England), 24*, 3551–3553.
Liu, C., Huang, C., & Chang, H. (2009). *Analytical Chemistry, 81*(6), 2383–2387.
Liu, D., Li, X., Zhou, J., Liu, S., Tian, T., Song, Y., ... Yang, C. (2017). *Biosensors & Bioelectronics, 96*, 332–338.
Ma, Y., Mao, Y., Huang, D., He, Z., Yan, J., Tian, T., ... Yang, C. J. (2016). *Lab on a Chip, 16*(16), 3097–3104.
Moneta, G. L. (2009). *Journal of Vascular Surgery, 2009*, 157–158.
Ren, W., Zhang, Y., Chen, H. G., Gao, Z. F., Li, N. B., & Luo, H. Q. (2016). *Analytical Chemistry, 88*(2), 1385–1390.
Ren, W., Zhang, Y., Huang, W. T., Li, N. B., & Luo, H. Q. (2015). *Biosensors & Bioelectronics, 68*, 266–271.
Saidur, M. R., Aziz, A. R., & Basirun, W. J. (2017). *Biosensors & Bioelectronics, 90*, 125–139.
Streets, D. G., Devane, M. K., Lu, Z., Bond, T. C., Sunderland, E. M., & Jacob, D. J. (2011). *Environmental Science & Technology, 45*(24), 10485–10491.
Tchounwou, P. B., Ayensu, W. K., Ninashvili, N., & Sutton, D. (2003). *Environmental Toxicology, 18*(3), 149–175.
Tian, T., An, Y., Wu, Y., Song, Y., Zhu, Z., & Yang, C. (2017). *ACS Applied Materials & Interfaces, 9*(36), 30480–30487.
Wang, Z., Heon Lee, J., & Lu, Y. (2008). *Chemical Communications (Cambridge, England), 45*, 6005–6007.
Wei, X., Tian, T., Jia, S., Zhu, Z., Ma, Y., Sun, J., ... Yang, C. J. (2016). *Analytical Chemistry, 88*(4), 2345–2352.
Xiong, Z., Liu, Q., Yun, W., Hu, Y., Wang, X., & Yang, L. (2019). *Analyst, 144*(17), 5143–5149.
Xu, X., Li, Y. F., Zhao, J., Li, Y., Lin, J., Li, B., ... Chen, C. (2015). *Analyst, 140*(23), 7841–7853.
Yun, W., Xiong, W., Wu, H., Fu, M., Huang, Y., Liu, X., & Yang, L. (2017). *Sens Actuators B Chem. 249*, 493–498.
Zhang, D., Gao, B., Chen, Y., & Liu, H. (2018). *Lab on a Chip, 18*(2), 271–275.
Zhang, D., Ma, B., Tang, L., & Liu, H. (2018). *Analytical Chemistry, 90*(3), 1482–1486.
Zhong, Y., Deng, C., He, Y., Ge, Y., & Song, G. (2015). *Analytical Methods, 7*(4), 1558–1562.